Short Papers

Measurements of Time-Varying Millimeter-Wave Vectors by a Dynamic Bridge Method

AILEEN M. YUREK, MEMBER, IEEE, M. G. LI, AND CHI H. LEE, MEMBER, IEEE

Abstract—**A dynamic bridge-measurement technique has been developed to characterize the time evolution of millimeter-wave fields in a plasma-controlled semiconductor waveguide. The time resolution of this technique is about 2 ns.**

I. Introduction

Recently, many plasma-controlled devices for switching [1], [2], modulating [3], [4], and phase shifting [1] millimeter-wave signals have been developed. These devices all incorporate balanced bridge techniques in which a plasma-controlled waveguide is placed in one arm of the bridge and a precision phase shifter and a precision attenuator are placed in the other arm [5]. A schematic of the millimeter-wave bridge is shown in Fig. 1. The millimeter-wave bridge is initially (with no plasma generation) balanced by adjusting the variable attenuator A and the phase shifter ϕ in arm b so that there is no signal at the output. When a plasma is generated in the semiconductor waveguide by electronic [5]–[7] or optical [1]–[4] means, a phase-shifted and/or amplitude-modulated millimeter-wave signal appears at the output of the bridge. Usually, the signal thus generated is of a transient nature with a characteristic decay time. The temporal variation of the signal depends upon the carrier transport dynamics. To understand the physics of wave–plasma interaction, it is necessary to have accurate measurements of the phase and amplitude of the millimeter-wave signal with subnanosecond time resolution. In other words, it requires a transient vector network analyzer with subnanosecond time resolution. This type of device is currently not available. In this paper, we report a new measurement technique that may fulfill this requirement.

II. Dynamic Bridge Technique

A dynamic bridge technique has been developed to determine the values of the plasma-induced phase and attenuation. This method exploits the fact that the temporal profile of the output of the bridge depends sensitively upon the initial phase angle between the electric fields in the two arms as well as upon the dynamics of the phase shift and attenuation due to the induced electron–hole plasma. This method has a large dynamic range; it is possible to follow the decay of the plasma density over four orders of magnitude.

To understand the dynamic bridge method, first consider a phasor diagram consisting of two interfering phasors representing

Manuscript received August 26, 1985; revised May 9, 1986. This work was supported in part by the U.S. Army Research Office and by the National Science Foundation.

A. M. Yurek was with the Department of Electrical Engineering, University of Maryland, College Park. She is now with the Optical Techniques Branch, Code 6570, Naval Research Laboratory, Washington, DC 20375-5000.

M. G. Li and C. H. Lee are with the Department of Electrical Engineering, University of Maryland, College Park, MD 20742.

IEEE Log Number 8610285.

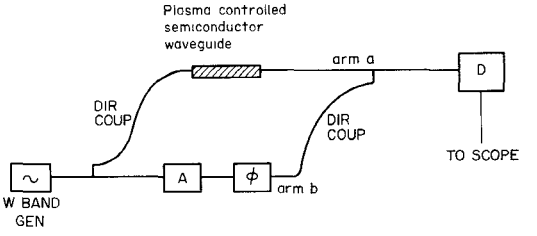

Fig. 1. Experimental arrangement to measure the dynamic evolution of the phase shift and attenuation in a plasma-controlled semiconductor waveguide.

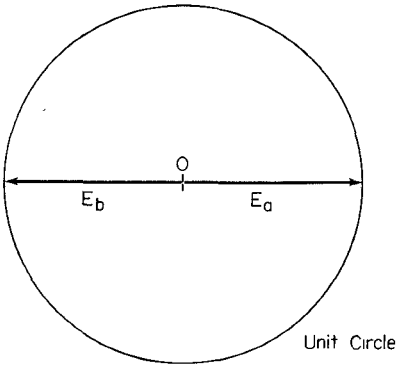

Fig. 2. Phasor diagram for the millimeter-wave bridge in the null condition. E_a represents the electric field in arm a of the bridge and E_b represents the electric field in arm b of the bridge.

the electric fields in the two arms of the bridge of Fig. 1. Let E_a represent the electric field in arm a and E_b represent the electric field in arm b. The output of the bridge is proportional to the magnitude of the resultant phasor. Since the millimeter waves must propagate in single-mode metal waveguides, they may be considered to be linearly polarized in the same direction. When the bridge is balanced before plasma generation, $E_a = -E_b$ and the output is zero. This situation is depicted in Fig. 2. When the bridge is deliberately set to be unbalanced by an angle ϕ, the initial condition is no longer zero but some resultant field E_r, as shown in Fig. 3. The magnitude of E_r may be calculated to be (assuming $E_a = E_b = 1$)

$$|E_r| = 2\left|\sin\frac{\phi}{2}\right|.$$

If a bridge imbalance is caused by plasma generation, the imbalance angle ϕ varies in time as shown in Fig. 4 due to the buildup and decay of plasma. We will ignore attenuation in this part of the discussion. As ϕ due to the plasma decreases, the phasor E_a rotates from its initial position OA along the circular arc $ABCG$ to its equilibrium position OG. The resultant phasors describing the output of the bridge at different instants in time are given by GB, GC, etc.

A more realistic situation is shown in Fig. 5. Here, the signal in arm a of the bridge follows the trajectory outlined by the points 1–5 of the figure. The magnitude of E_a is indicated by the length of the vector E_a (dotted lines), and the phase change is the

0018-9480/86/1100-1220$01.00 ©1986 IEEE

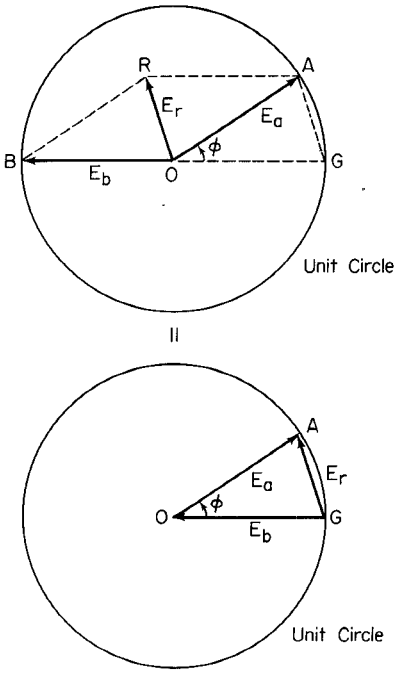

Fig. 3. Phasor diagram for the unbalanced bridge. A simple geometric construction is used to find the resultant phasor E_r.

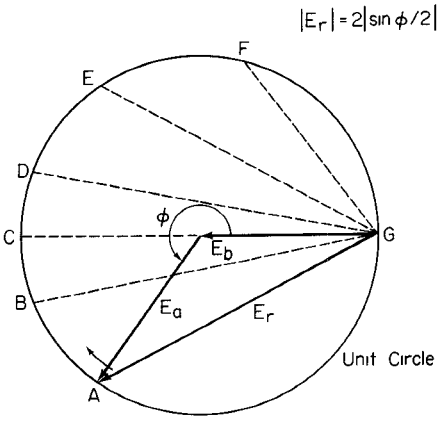

Fig. 4. Phasor diagram showing the variation of the resultant electric field E_r due to a "plasma-induced" phase shift.

difference in angle from the initial condition. Fig. 5(a) and (b) show the variation of the resultant phase E_r for two different initial phase offsets; (a) contains an initial offset of 0° (the two arms adding) and (b) contains an initial offset of 90°. Note that the variation of E_a along the trajectory in time is the same for both cases. Also note that experimentally E_b is fixed, E_a varies, and $|E_r|$ is the measurable quantity. By knowing the two initial phase offsets, the variation of the magnitude of E_r may be found from the measured output of the bridge. Fig. 6 shows the construction used to find the points of the trajectory taken by E_a as a function of time. Knowing the magnitude of $E_{r_{0°}}$ and $E_{r_{90°}}$ at any given time after the plasma is generated, a circular arc is drawn centered at point A with a radius $E_{r_{0°}}$, and another circular arc is drawn centered at point B with a radius $E_{r_{90°}}$. The intersection of these two arcs determines a point of the trajectory. The relative attenuation at any time is found from the distance from the corresponding point on the trajectory to the origin, and the relative phase is found in the same manner as the case where attenuation was ignored.

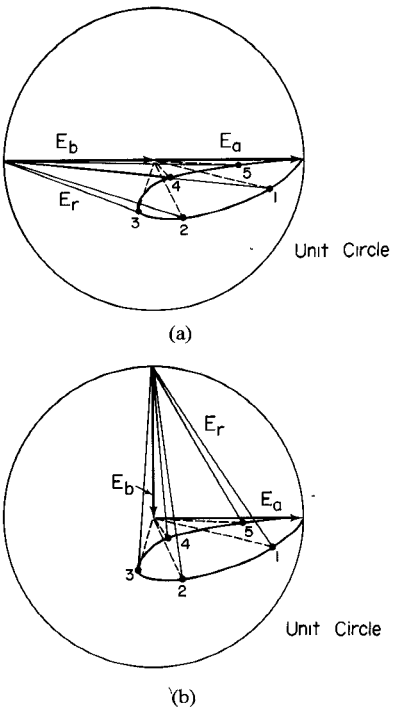

Fig. 5. Phasor diagram representing an actual variation of E_a and E_r for two different initial phase offsets. (a) Initial offset of 0°. (b) Initial offset of 90°.

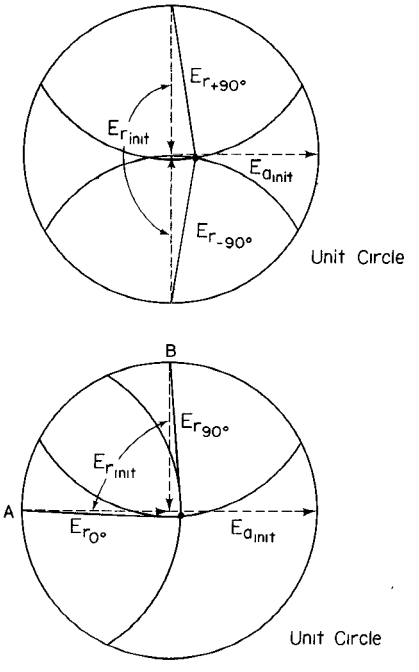

Fig. 6. Construction showing how the magnitude and phase of E_a may be found knowing the variation of E_r for two initial phase offsets; in this case, 0° and 90°

The initial offsets chosen are purely arbitrary; any two initial phase offsets should give the same result. However, the case of 0° and 90° initial offsets has some advantages from an experimental point of view. When there is a large attenuation, the phasor E_a is very short. Fig. 6 shows a comparison of the geometrical construction for the cases of +90° and −90° initial offsets and 0° and 90° initial offsets and large attenuation. Note that the intersection of the two circular arcs is much clearer in the 0° and 90° initial offsets case. What is illustrated in Fig. 6 is not really a

geometrical construction problem; in both of these cases, it is easy to calculate the magnitude and phase of E_a without doing any geometrical construction. It turns out that in the case of $+90°$ and $-90°$ initial offsets, a very small error in taking data causes the two arcs not to intersect at all. The case of 0° and 90° initial offsets also has errors inherent in taking data, but averaging the results from several different initial phase offset cases can eliminate this error.

III. Results

An example of the temporal variation of phase and loss in a silicon waveguide illuminated by a 200-ns pulse from a GaAs diode laser is shown in Fig. 7. The frequency of the millimeter waves is 94 GHz and they are propagating in the TE_{01} mode. Here, the data taken with the dynamic bridge method are compared with a theoretical curve and data taken by a nulling method [8]. The nulling method requires that the source generating the plasma be stable and have a repetition rate fast enough to trigger an oscilloscope in the automatic mode. It consists of using the variable phase shifter and the variable attenuator to null the millimeter-wave bridge at any time after the plasma is generated. The dynamic bridge method is most useful in a situation where the repetition rate of the plasma generation is slow or the amount of plasma generated varies from pulse to pulse. The temporal resolution of the dynamic bridge method is limited by the resolution of the detection system. In our case, it is about 2 ns, the response time of the oscilloscope.

A detailed description of the comparison between the experimental results and theoretical calculation has been given in [9]. The theoretical model calculates the variation in amplitude and phase of the millimeter waves as a function of time after the onset of laser illumination. It takes into account the laser pulse shape and the diffusion of the plasma into the bulk silicon during and after the laser pulse. The emphasis here is on the good agreement between the experimental data obtained by two different methods. From Fig. 7, it is clear that the theoretical and experimental curves agree very well except for the phase shift in the range from 5 to 50 μs. This discrepancy is probably due to a combination of two factors: first, the fact that the plasma depth and density were assumed to be spatially abrupt and constant, respectively, and second, that the model used to determine the phase shift and attenuation predicts a cutoff of the lowest order mode which does not actually occur. Because the condition of the waveguide in this time range is near the "cutoff" condition, the theoretical prediction there may not be accurate.

If the laser has a low repetition rate and is not very reproducible from shot to shot, only the dynamic bridge method is applicable. This was the case when a frequency doubled mode-locked Nd:YAG laser was used to illuminate the same silicon waveguide. The laser delivered a single pulse in every shot with a duration of 30 ps at 530 nm. The 30-ps green pulse has an average energy of 42 μJ and an absorption depth in silicon of 1 μm, and it generated a plasma of density 5×10^{19} cm^{-3}. As a comparison, the pulse energy of the GaAs diode laser used was only 0.2 μJ and the absorption depth of the GaAs laser radiation in silicon is 29 μm. The carrier density generated in silicon was thus only 2×10^{16} cm^{-3}. The 30-ps laser pulse could be regarded as a delta function exciting source since the pulse width was much shorter than the carrier lifetime. With such an intense and instantaneous excitation of silicon, one expects instantaneous phase shift and attenuation of millimeter waves due to the instantaneous generation of electron–hole plasma in the silicon waveguide. The phase shift and attenuation of the millimeter

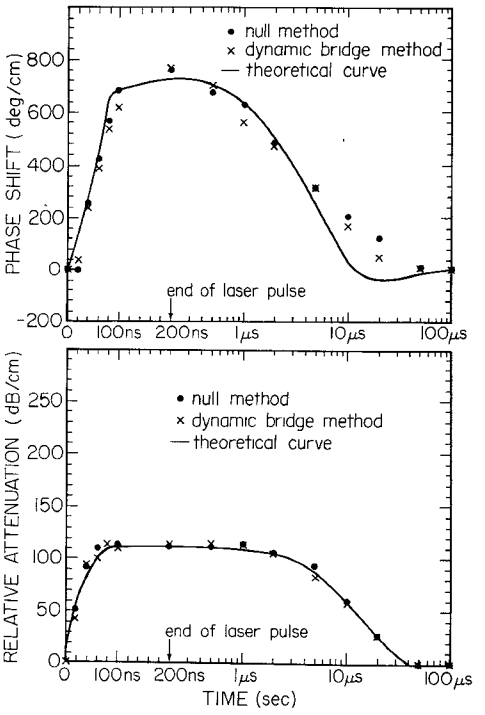

Fig. 7. Comparison of the dynamic bridge data with the nulling method data and a theoretical model for a 1.0×0.5-mm silicon waveguide illuminated by a 900-nm GaAs diode laser. The upper curve is phase shift with respect to time; the lower curve is relative attenuation with respect to time. Note that the time scale is linear for the first 200 ns, the duration of the laser pulse.

waves should remain constant for a period of time and begin to vary with time as the plasma starts to decay. We have used the dynamic bridge method to monitor the change of phase shift and attenuation of the millimeter waves immediately following the excitation by the laser pulse.

A comparison of the theoretical model and the experimental results obtained by using the dynamic bridge method alone is shown in Fig. 8. Here, the recombination time was fitted at 20 μs, and the ambipolar diffusion coefficient was held at a constant 18 cm^2/s. The initial plasma density was fitted at 10^{18} cm^{-3}, an order of magnitude less than the plasma density inferred from measurements of the laser energy. One reason for this discrepancy is that the complete theoretical model assumes an abrupt junction between the plasma layer and the rest of the waveguide. From the steady-state model [9], it can be seen that the millimeter waves begin to interact with the plasma in the density range from 10^{14} to 10^{16} cm^{-3}, depending upon the plasma depth. The plasma layer model chooses an average plasma depth and density which is spatially abrupt. This model ignores the plasma in the tail of the distribution, which for large total plasma densities may be significant. These smaller plasma densities at larger plasma depths interact with millimeter waves, producing larger attenuations than those predicted by the abrupt junction model. The large peak in the theoretical attenuation curve in Fig. 8 is probably due to the fact that the model of the waveguide used [9] predicts a cutoff waveguide size for the lowest order semiconductor waveguide mode. This "cutoff" never occurs in reality. In the theoretical model, as the plasma is diffusing into the semiconductor waveguide, the waveguide is becoming pinched off. The predicted attenuation in the near-pinchoff case is probably too high due to the model predicting an actual cutoff condition.

In conclusion, a dynamic bridge measurement technique has been developed to characterize the behavior of plasma-controlled

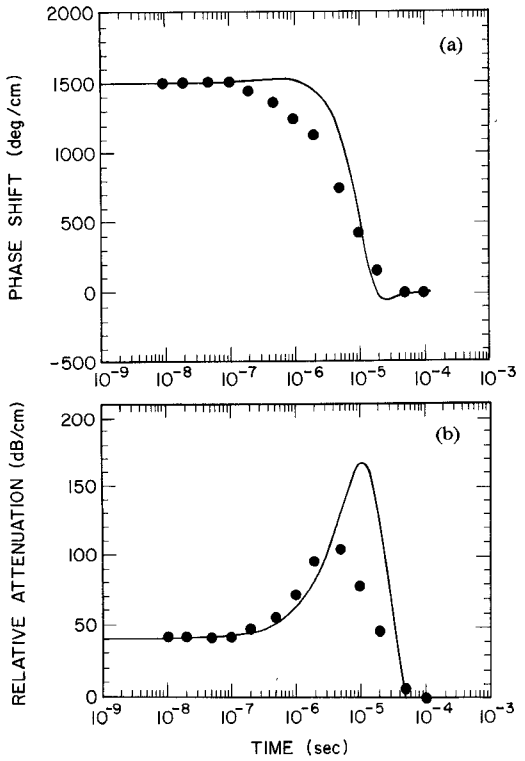

Fig. 8. Comparison of theoretical (solid line) and experimental (data points) results for the situation when the millimeter-wave bridge is illuminated by a single pulse from a frequency doubled mode-locked Nd:YAG laser. The experimental technique is the dynamic bridge method. (a) Phase shift with respect to time. (b) Relative attenuation with respect to time.

semiconductor waveguides. This technique is also applicable to the measurement of the transient behavior of any microwave/millimeter-wave device. The time resolution of this technique can be further improved to the picosecond range if an optoelectronic correlation or an electronic sampling technique is used to map out the temporal variation of the signal [10].

References

[1] C. H. Lee, P. S. Mak, and A. P. DeFonzo, "Optical control of millimeter-wave propagation in dielectric waveguides," *IEEE J. Quantum Electron.*, vol. QE-16, pp. 277–288, 1980.

[2] W. Platte, "Optoelectronic microwave switching via laser-induced plasma layers in GaAs microstrip section," *IEEE Trans. Microwave Theory Tech.*, vol. MTT-29, p. 1010, 1981.

[3] M. G. Li, W. L. Cao, V. K. Mathur, and C. H. Lee, "Wide bandwidth, high repetition rate optoelectronic modulation of millimeter-waves in GaAs waveguide," *Electron. Lett.*, vol. 18, pp. 454–456, 1982.

[4] K. Ogusu, "New dielectric waveguide structure for millimeter-wave optical control," *Electron. Lett.*, vol. 19, pp. 253–254, 1983.

[5] H. Jacobs and M. M. Chrepta, "Electronic phase-shift for millimeter-wave semiconductor dielectric integrated circuit," *IEEE Trans. Microwave Theory Tech.*, vol. MTT-22, pp. 411–417, 1974.

[6] G. H. Novick, C. M. LoCasio, and J. Londono, "Nonresonant semiconductor phase shifter," *IEEE Trans. Microwave Theory Tech.*, vol. MTT-30, pp. 2034–2036, 1982.

[7] R. E. Horn, H. Jacobs, K. L. Klohn, and E. Friebergs, "Single frequency electronic modulated analog line scanning using a dielectric antenna," *IEEE Trans. Microwave Theory Tech.*, vol. MTT-30, pp. 816–820, 1982.

[8] A. M. Yurek, "Millimeter-wave technique for characterizing the behavior of optically induced plasmas in semiconductor waveguides," Ph.D. dissertation, University of Maryland, 1984.

[9] A M. Yurek, C. D. Striffler, and C. H. Lee, "Optoelectronic devices for millimeter waves," ch. 4 in *Infrared and Millimeter Waves*, vol. 14, K. Button, Ed. New York: Academic Press, 1985.

[10] C. H. Lee, A. M. Yurek, M. G. Li, E. Chauchard, and R. P. Fischer, "Optoelectronic modulation of millimeter waves in a silicon-on-sapphire waveguide," in *Tech. Dig., Topical Meeting on Picosecond Electronic and Optoelectronics* (Incline Village, NV) paper WE4, March 13–15, 1985.

An *X*-Band Four-Diode Power Combiner Using Gunn Diodes

K. BHATTACHARYYA, S. K. DE, G. GHOSH, P. C. RAKSHIT, P. K. SAHA, AND B. R. NAG

***Abstract*—A four-diode *X*-band Gunn diode combiner is described, and the performance characteristics are presented for combining efficiency, tuning range, pushing figure, frequency drift, external *Q*, and FM noise.**

I. Introduction

Solid-state microwave sources are advantageous in many applications since the size is small and the required power supplies are simple. The maximum power available from an individual device is, however, limited to 500–750-mW CW for Gunn diodes in the *X*-band [1]. Although higher power may be obtained from IMPATT diodes, Gunn diodes are often preferred for certain purposes because of their lower noise [2]. Attempts have, therefore, been made for generating higher powers than obtainable from single devices by combining the outputs of several devices [3].

A general scheme for combining multiple diodes in a rectangular cavity was given by Kurokawa and Magalhaes [4]. A cylindrical cavity combiner using the same principles, developed by Harp and Stover [5], is widely used. A variation of this scheme, proposed by Diamond [6], uses modules of diode pairs in push–pull operation and thereby achieves higher packing density and combining efficiency than a regular cylindrical cavity combiner. These types of combiners, however, require precise design and adjustments for realizing the optimum performance. Simple forms of combiners with less stringent design requirements are, therefore, preferred for a small number of diodes. Simple single-resonator two-diode combiners have been reported with different configurations [7], [8].

Single-resonator, four-diode combiners have also been reported in two configurations [9], [10]. In one configuration [9], the diodes are mounted at the four corners of a TE_{101} rectangular cavity. The output is coupled through an iris and the tuning is achieved by a dielectric screw tuner. It is reported that combining efficiencies of 80–90 percent and a tuning bandwidth of 3 GHz at 33 GHz may be realized with these combiners. In the second configuration [10], modules of two-diode combiners are mounted in cascade in an oversized shorted waveguide. The discontinuity at the output end and the short forms the cavity, and tuning is achieved by adjusting the position of the short.

In this paper, a simpler single-resonator, four-diode combiner is described, which is suitable for the *X*-band. This configuration has been mentioned in a footnote in [11] but the details are not available. The performance characteristics of the combiner using diodes with different power ratings are also presented.

II. The Combiner and Performance Characteristics

The mounting arrangement of the diodes in the combiner is shown schematically in Fig. 1. The diodes are mounted at the opposite ends of two posts, placed symmetrically on the two sides of the central line in a cross-sectional plane of a shorted, rectan-

Manuscript received March 19, 1986; revised June 17, 1986. This work was supported in part by the Defence Research and Development Organization, Ministry of Defence, Government of India.

The authors are with the Institute of Radio Physics and Electronics, 92, Acharya Prafulla Chandra Road, Calcutta-700 009 India.

IEEE Log Number 8610288.

0018-9480/86/1100-1223$01.00 ©1986 IEEE